Inertial Effects of a Small Brownian Particle Cause a Colored Power Spectral Density of Thermal Noise

Anita Jannasch, Mohammed Mahamdeh, and Erik Schäffer*

Nanomechanics Group, Biotechnology Center, TU Dresden, Tatzberg 47-51, 01307 Dresden, Germany

(Received 18 August 2011; published 21 November 2011)

The random thermal force acting on Brownian particles is often approximated in Langevin models by a ''white-noise'' process. However, fluid entrainment results in a frequency dependence of this thermal force giving it a ''color.'' While theoretically well understood, direct experimental evidence for this colored nature of the noise term and how it is influenced by a nearby wall is lacking. Here, we directly measured the color of the thermal noise intensity by tracking a particle strongly confined in an ultrastable optical trap. All our measurements are in quantitative agreement with the theoretical predictions. Since Brownian motion is important for microscopic, in particular, biological systems, the colored nature of the noise and its distance dependence to nearby objects need to be accounted for and may even be utilized for advanced sensor applications.

DOI: 10.1103/PhysRevLett.107.228301 PACS numbers: 05.40.Jc, 05.40.Ca, 82.70.Dd, 87.80.Cc

The thermal agitation of fluids leads to the random, jiggling motion of suspended particles known as Brownian motion. In the Ornstein-Uhlenbeck theory of Brownian motion, the motion is a purely random, Markovian—i.e., memoryless—Gaussian process with ''white noise'' [1,2]. White noise implies that the noise intensity, i.e., the power spectral density (PSD) of the noise term in a Langevin model, does not depend on frequency; its PSD is flat or constant. ''Color'' is introduced to the noise by the fluid entrainment of the particle [3–7]. Through its motion, the particle accelerates the entrained fluid [8]. This acceleration depends on the past motion of the particle and introduces an inertial memory effect. In the equation of motion, this non-Markovian process is reflected by a frequency-dependent thermal force which fulfills the fluctuation-dissipation theorem [4–6]. In analogy to filtering white light, this frequency-dependent fluctuation process is often called ''colored noise'' [2]. Through simulations of Brownian particle motion, the colored-noise effect became evident as a $t^{-3/2}$-power-law tail at long times of the velocity autocorrelation [9]. Equivalently, the noise intensity is expected to scale with the square root of the frequency $f^{1/2}$ when a confined particle's position PSD is analyzed [10]. The effect is theoretically well established, but, since it is small, it has not been measured directly [10].

To directly measure the color of thermal noise of classical Brownian motion, i.e., in an incompressible fluid, we used a very stable and strong optical trap [11,12] in combination with highly efficient probes: antireflection-coated titania microspheres [13–15]. A trapped microsphere is typically described by an overdamped harmonic oscillator with a relaxation time $\tau = \gamma/\kappa$ with the microsphere drag coefficient γ and the Hookean spring constant or trap stiffness κ. The efficient titania probes enabled us to achieve a large trap stiffness and, therefore, a small relaxation time or large characteristic frequency $f_c = 1/(2\pi\tau)$. For frequencies $f \ll f_c$, inertial and viscous forces can be neglected in the equation of motion (see below, [10]). Then the optical force $F_{\text{optical}} = \kappa x$ directly balances the random, thermal force $F_{\text{thermal}} = F_{\text{optical}}$. Thus, in this limit, the displacement x in a strong, calibrated optical trap is a direct measure for the thermal force and its dependence on the frequency and distance to a nearby surface [10,16]. Here, we measured this dependence and found quantitative agreement between theory and experiment.

The optical trap has been described in detail previously [11,12]. Briefly, an infrared laser (5 W at 1064 nm) was expanded (filling factor $\alpha = 2.0$ [12]) and guided through various optics to the trapping objective. This objective focused the beam to a diffraction limited spot with 1.05 W power [12]. In the laser focus, small dielectric particles can be trapped. The light scattered by such a particle was collected by a second, identical objective and projected onto a quadrant photodiode (QP154-Q-HVSD, Pacific Silicon Sensors, Westlake Village, CA, optimized for 1064 nm, $U_{\text{bias}} = 110$ V) for back-focal-plane detection [17,18]. The sampling rate was 1.25 MHz (NI PXI-6251, National Instruments, Austin, TX). The temperature of the two objectives was kept constant at $33.000 \pm 0.001\,^{\circ}\text{C}$ [11]. The sample chamber—mounted between the two temperature-controlled objectives using a 1.518-refractive-index immersion oil (unless noted otherwise)—was composed of two cover slips (18 and 22 mm^2) separated by two Parafilm® stripes forming a $3 \times 18 \times 0.1$ mm^3 channel sealed with nail polish. The sample position was controlled in three dimensions by a piezoelectric nanopositioning system [11]. The antireflection-coated titania microspheres [15] had a diameter of 1.00 ± 0.04 μm and were suspended in aqua bidestillata (18.2 MΩ cm). Calibration was done using a combined PSD and drag-force

method using a small sinusoidal excitation of the trapped microsphere via the sample stage [16,19]. Since the driving amplitude and theoretical response of the microsphere are known, all three unknown system parameters can be measured: the displacement sensitivity β (voltage-to-meter conversion factor of the photodiode), the trap stiffness κ, and the drag coefficient γ of the microsphere. We determined the absolute microsphere-center–surface distance ℓ by first bringing the microsphere into contact with the surface and then moving a controlled distance away from the surface using the nanopositioning stage. Taking the focal shift into account [19], we estimate ℓ to be accurate within ± 0.25 μm. For the largest distance (see below), we used a long-range travel piezoinertial drive [11] resulting in an accuracy for ℓ of ± 1 μm.

To quantitatively measure the small colored-noise effect, we optimized the experimental conditions to minimize drift. At low frequencies, our measurements were limited by $1/f$ noise. At high frequencies, the characteristic frequency f_c of the trapped particle was limiting. Slow drift sometimes affected the whole frequency range, e.g., due to fluctuations of the detector sensitivity or the room temperature. Since the magnitude of the colored-noise effect was on the percent level, drift and resolution of the measurement had to be smaller. To reach a $N^{-1/2} = 1\%$ precision in a power spectral analysis, at least $N = 10\,000$ power spectra have to be averaged [10,20]. To acquire enough power spectra in a time window that is not affected by drift, we decreased the frequency resolution of the measurement and, therefore, the total measurement time t_{msr}. Our system was stable over 500 s such that we achieved a 0.3% rms-noise level ($N = 100\,000$) with a 200 Hz resolution. In this time period, the magnitude of drift was less than the relative displacements in the trap. For a strong trap, the displacements were on the order of 1 pm/$\sqrt{\mathrm{Hz}}$ (Fig. 1) imposing stringent stability conditions on the apparatus. To ensure that our measurements were not affected by drift, we acquired one 12.5-s-long calibration spectrum before and after each long-duration, high-precision measurement (Fig. 1). Only if the two calibration spectra, the high-precision spectrum, and the according fits to the data agreed within error bars, the drift was low enough. In this manner, we acquired high-precision power spectra as a function of distance from the surface. To trap at the largest distance, ≈ 20 μm from the surface, we used an immersion oil with a refractive index of 1.53 to compensate for spherical aberrations [12,19,21]. At this distance, we could acquire only $N = 10\,000$ spectra; our measurements were limited by low-frequency noise presumably due to laser heating [22] and subsequent convective currents [23].

The measured power spectra were in quantitative agreement with the theoretical predictions. The Langevin equation of motion for the position $x(t)$ of the trapped microsphere with radius R and mass m moving parallel to a surface at a distance ℓ from the microsphere center is $m\ddot{x} + \gamma(f, R/\ell)\dot{x} + \kappa x = F_{\mathrm{thermal}}$ with the thermal noise $F_{\mathrm{thermal}}(f) = [2k_BT\,\mathrm{Re}\{\gamma(f, R/\ell)\}]^{1/2}\xi(f)$ [10]. The white-noise process is characterized by $\langle\xi(t)\rangle = 0$ and $\langle\xi(t)\xi(t')\rangle = \delta(t - t')$ where δ is Dirac's delta function and $\langle\cdots\rangle$ denotes the expectation value. The hydrodynamically correct one-sided PSD for the microsphere's position with Fourier transform $\tilde{x}(f)$ is then given by [16,24]

$$P_\ell(f) = \langle|\tilde{x}(f)|^2\rangle = \frac{(D_0/\pi^2)\,\mathrm{Re}\{\gamma/\gamma_0\}}{(f_c + f\,\mathrm{Im}\{\gamma/\gamma_0\} - f^2/f_m)^2 + (f\,\mathrm{Re}\{\gamma/\gamma_0\})^2}. \quad (1)$$

The frequency- and distance-dependent drag coefficient is Padé approximated to [16]

$$\gamma(f, R/\ell) = \frac{\gamma_0[1 + (1-i)\sqrt{f/f_\nu} - i(2/9)(f/f_\nu)]}{1 - (9/16)(R/\ell)\{1 - (1/3)(1-i)\sqrt{f/f_\nu} + i(2/9)(f/f_\nu) - (4/3)[1 - \exp(-(1-i)[(2\ell/R) - 1]\sqrt{f/f_\nu})]\} + \cdots}, \quad (2)$$

where $\gamma_0 = 6\pi\eta R$ is the Stokes drag coefficient with the viscosity η. The diffusion coefficient far away from the surface is $D_0 = k_BT/\gamma_0$ with the Boltzmann constant k_B and the temperature T. There are three characteristic frequencies for (i) the PSD corner $f_c = \kappa/(2\pi\gamma_0)$, inertial effects due to (ii) the mass $f_m = \gamma_0/(2\pi m)$, and (iii) viscous entrainment $f_\nu = \nu/(\pi R^2)$ where $\nu = \eta/\rho$ is the kinematic viscosity with the liquid density ρ. Re and Im are the real and imaginary part of a complex number, respectively. Note that the numerator of Eq. (1) is directly proportional to the PSD of the noise term. The f scaling of this colored noise is discussed in the next paragraph. We fitted Eq. (1) in the range of 1–100 kHz to the PSD data acquired at different distances from the surface, normalized the PSD by its extrapolated, fit-based value at $f = 0$, and subtracted 1 (Fig. 2). The resulting fit parameters are listed in Table I. The displacement sensitivity was calculated from the power in the "calibration peak" (Fig. 1). The measured temperature [26] increased with distance from the surface [gray diamonds, inset Fig. 2(a)]. This increase was due to laser heating and the surface acting as a heat sink—in quantitative agreement with a

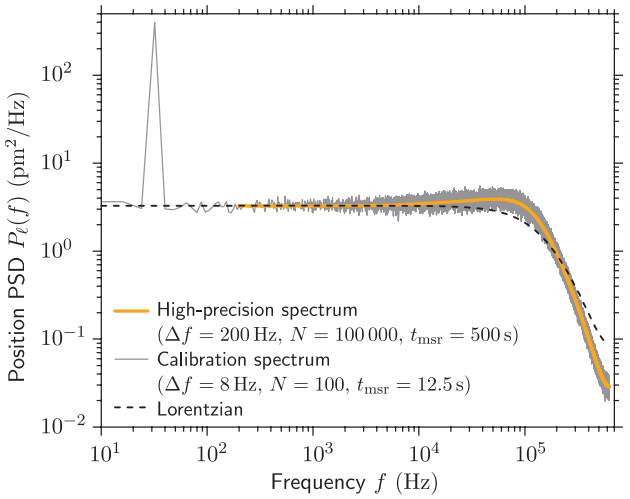

FIG. 1 (color). "High-precision" and "calibration" position power spectral density (PSD) of an antireflection-coated titania microsphere held in an optical trap at a distance $\ell/R = 12$ from the surface. The calibration (gray line) and high-precision (orange line) spectrum shown are the average of 100 and 100 000 independent power spectra, respectively. On the scale of the figure, fits of Eq. (1) to the data (not shown) are indistinguishable from the high-precision spectrum. The calibration spectrum with a $\Delta f = 8$ Hz frequency resolution features a peak at the 32 Hz stage driving frequency used for calibration [16]. A Lorentzian (dashed line) is plotted for comparison. Deviations from the Lorentzian are due to the "colored-noise" intensity of the thermal force. Aliasing and bias are accounted for in the fits [20,32].

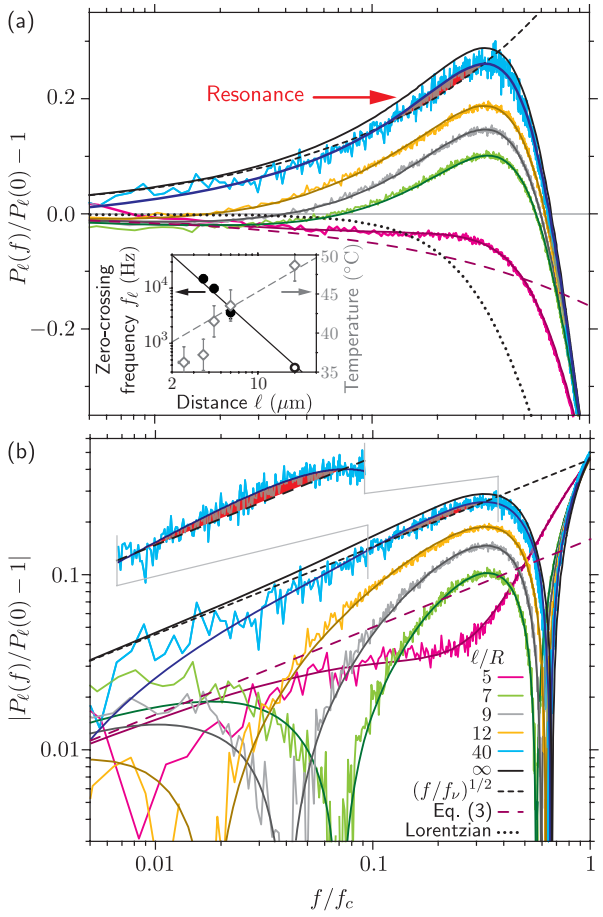

FIG. 2 (color). High-precision power spectra as a function of microsphere-center–surface distance ℓ/R on (a) a semilog and (b) the absolute value on a log-log scale. Smooth solid lines are fits of Eq. (1) to the data. The parameters are given in Table I. Equation (1) for $\ell/R \to \infty$ (black solid line), a Lorentzian (black dotted line), and the positive and negative square-root scaling $\sqrt{f/f_\nu}$ (black short-dashed line) and Eq. (3) (magenta long-dashed line for $\ell/R = 5$), respectively, are drawn for comparison. The frequency axis was scaled by the corner frequency f_c because (i) three different microspheres were used, (ii) temperatures, and (iii) distances differed. The red-shaded area is a resonant enhancement of the colored-noise intensity. Inset: Zero-crossing frequency [black solid (open) circles based on data (fit)], $f_\ell = \nu/(2\pi\ell^2)$ (black solid line), temperature (gray diamonds, Table I), and temperature model (gray dashed line, [22]) as a function of distance ℓ.

model (gray dashed line) with no adjustable parameters [22]. Over the fitted range and for all distances, Eq. (1) deviated on average less than $\sqrt{\chi^2_{\rm red}/N} \lesssim 1\%$ from the experimental PSD (see Table I).

The magnitude and scaling with frequency of the colored-noise intensity strongly depended on the distance to the surface (Fig. 2). In the limit of $\ell/R \to \infty$, a Taylor expansion in frequency around $f = 0$ of the PSD [Eq. (1)] results to lowest order in $P_{\ell=\infty}(f)/P_{\ell=\infty}(0) = 1 + \sqrt{f/f_\nu} + \cdots$ [10]. Thus, far away from the surface, the color of the noise intensity scales with the square root of the frequency and only depends on the particle size and the *kinematic* viscosity—it is an *inertial* effect of the entrained fluid [10]. This scaling is plotted in Fig. 2 with a black short-dashed line. For *finite* values of ℓ/R, the resulting scaling is

$$P_\ell(f)/P_\ell(0) = 1 - \frac{\sqrt{f/f_\nu}}{2[1 - (9/16)(R/\ell)]} + \cdots. \qquad (3)$$

Interestingly, in this case, the colored part of the noise intensity depends on ℓ and is negative. For a low enough bandwidth, this sign reversal means that noise is suppressed due to the entrained fluid and coupling to the surface. We indeed observed such a suppression up to a characteristic frequency f_ℓ at which a zero crossing occurred in the normalized plot of Fig. 2. The frequency of these zero crossings [black circles, inset Fig. 2(a)] scaled with ℓ^{-2} and was well approximated by an estimate of $f_\ell \approx \nu/(2\pi\ell^2)$ [black solid line, inset Fig. 2(a), [27]]. The negative-square-root scaling of the colored noise according to Eq. (3) was approached for the $\ell/R = 5$ data (magenta long-dashed line in Fig. 2). The positive-square-root scaling (black short-dashed line in Fig. 2) was nearly reached for our $\ell/R = 40$ data set. However, even at this distance, there was still a significant deviation from the scaling

TABLE I. Fit parameters of Eq. (1) for the data shown in Fig. 2. Constant parameters were the microsphere diameter $R = 0.51\ \mu$m, its density $\rho_{\text{titania}} = 2500\ \text{kg m}^{-3}$ [25], the water density $\rho = 1000\ \text{kg m}^{-3}$, the distance ℓ, and the number of averaged power spectra $N = 100\,000$. In addition, we used a low pass with filter frequency $f_{3\ \text{dB}} = 360$ kHz to account for the finite bandwidth of the photodiode [20].

ℓ/R	f_c (kHz)	D^{volt} (V^2/s)[a]	β (nm/V)	T (°C)[b]	χ^2_{red}[c]
5	71.54 ± 0.02	1010 ± 1	23.59 ± 0.01	36	1.21
7	148.2 ± 0.1	1402 ± 2	20.61 ± 0.02	37	1.07
9	156.9 ± 0.2	1485 ± 3	21.15 ± 0.03	42	1.13
12	155.7 ± 0.2	1484 ± 4	21.81 ± 0.03	44	1.59
40[d]	181.0 ± 0.8	1820 ± 20	21.12 ± 0.09	49	1.11

[a] $D_0 = \beta^2 D^{\text{volt}}/[1 - (9/16)(R/\ell)]$.
[b] The standard error of the temperature was dominated by the error of the microsphere size amounting to about ±2 °C.
[c] Based on the number of fitted data points, the standard error of the reduced chi-squared value is ±0.06.
[d] $N = 10\,000$.

behavior expected at infinite distance (black solid line in Fig. 2).

For this largest distance, we measured a small resonant enhancement of the colored-noise intensity. For $f_c \to f_\nu$, the harmonic oscillator is not overdamped anymore. This results in a resonance which shows up as increased noise beyond the positive-square-root scaling [28]. The red-shaded area in Fig. 2 marks this small, but significant, resonant enhancement. To enhance this effect even further, f_ν/f_c needs to be decreased. Since for our setup f_c was already maximized and our microsphere size was fixed [15], we reduced the kinematic viscosity. However, excessive heating of various liquids precluded such experiments.

In conclusion, we directly measured the colored nature of the thermal noise of Brownian motion. By the scaling of the noise amplitude with $(f/f_\nu)^{1/2}$, we could confirm that the origin of this colored noise was due to the acceleration of the entrained fluid, i.e., an inertial effect. Furthermore, the strong dependence of the colored-noise amplitude and scaling on the distance may open up the possibility to use the effect as a sensitive means to determine the presence of far away objects. Since the frequency f_ℓ at which the sign reversal occurred scaled with ℓ^{-2}, this frequency may be used as a sensitive indicator. Brownian motion is key to biological systems. Thus, the colored nature of the underlying noise process—and, in particular, its dependence on distance—may play a significant role in the crowded cellular environment. Furthermore, for sensitive biophysical measurements (e.g., [24,29,30]) the effect has to be accounted for. The resonance—once enhanced further—may even be exploited for advanced force spectroscopy measurements. Finally, other colors of noise are often based on the frequency of visible light [31]. Since the here-discussed noise has a weak, square-root dependence on frequency resulting in a lower frequency band than, for example, blue noise ($\propto f$), we suggest the color of thermal noise of Brownian motion to be yellow.

We thank members of the Nanomechanics group, J. Howard, F. Jülicher, S. W. Grill, and S. F. Nørrelykke for comments on the manuscript. The work was supported by the Deutsche Forschungsgemeinschaft (DFG; Emmy Noether Program), European Research Council (ERC Starting Grant 2010), and the Technische Universität Dresden.

*To whom correspondence should be addressed.
Erik.Schaeffer@biotec.tu-dresden.de

[1] G. E. Uhlenbeck and L. S. Ornstein, Phys. Rev. **36**, 823 (1930).
[2] P. Hänggi and P. Jung, in *Advances in Chemical Physics* (John Wiley & Sons, New York, 2007), Vol. 89, pp. 239–326.
[3] R. F. Fox and G. E. Uhlenbeck, Phys. Fluids **13**, 1893 (1970).
[4] T. S. Chow and J. J. Hermans, J. Chem. Phys. **56**, 3150 (1972).
[5] E. H. Hauge and A. Martin-Löf, J. Stat. Phys. **7**, 259 (1973).
[6] D. Bedeaux and P. Mazur, Physica (Amsterdam) **76**, 247 (1974).
[7] Y. Pomeau and P. Résibois, Phys. Rep. **19**, 63 (1975).
[8] L. Landau and E. Lifshits, *Fluid Mechanics*, Course of Theoretical Physics Vol 6 (Butterworth-Heinemann, Oxford, 1987).
[9] B. J. Alder and T. E. Wainwright, Phys. Rev. Lett. **18**, 988 (1967).
[10] K. Berg-Sørensen and H. Flyvbjerg, New J. Phys. **7**, 38 (2005).
[11] M. Mahamdeh and E. Schäffer, Opt. Express **17**, 17 190 (2009).
[12] M. Mahamdeh, C. P. Campos, and E. Schäffer, Opt. Express **19**, 11 759 (2011).
[13] V. Bormuth, A. Jannasch, M. Ander, C. Katz, A. van Blaaderen, J. Howard, and E. Schäffer, Opt. Express **16**, 13 831 (2008).
[14] A. Jannasch, V. Bormuth, C. van Kats, A. van Blaaderen, J. Howard, and E. Schäffer, Proc. SPIE Int. Soc. Opt. Eng. **7038**, 70382B (2008).
[15] A. F. Demirörs, A. Jannasch, P. D. J. van Oostrum, E. Schäffer, A. Imhof, and A. van Blaaderen, Langmuir **27**, 1626 (2011).
[16] S. F. Tolić-Nørrelykke, E. Schäffer, J. Howard, F. Pavone, F. Jülicher, and H. Flyvbjerg, Rev. Sci. Instrum. **77**, 103101 (2006).
[17] F. Gittes and C. F. Schmidt, Opt. Lett. **23**, 7 (1998).
[18] A. Pralle, M. Prummer, E. L. Florin, E. H. K. Stelzer, and J. K. H. Hörber, Microsc. Res. Tech. **44**, 378 (1999).
[19] E. Schäffer, S. Nørrelykke, and J. Howard, Langmuir **23**, 3654 (2007).
[20] K. Berg-Sørensen and H. Flyvbjerg, Rev. Sci. Instrum. **75**, 594 (2004).
[21] S. N. Reihani and L. B. Oddershede, Opt. Lett. **32**, 1998 (2007).

[22] E. Peterman, F. Gittes, and C. F. Schmidt, Biophys. J. **84**, 1308 (2003).
[23] H. Mao, J. R. Arias-Gonzalez, S. B. Smith, I. Tinoco, and C. Bustamante, Biophys. J. **89**, 1308 (2005).
[24] S. M. van Netten, J. Acoust. Soc. Am. **89**, 310 (1991).
[25] The density of the shell was based on the amount of shrinkage observed by transmission electron microscopy of as-prepared-titania microspheres upon sintering [15]. The density of the anatase-titania core was $\rho_{\text{titania}} = 4200\ \text{kg m}^{-3}$. The core-shell density was calculated by the total mass of core and shell divided by the total volume.
[26] Since the calibration depends on the absolute temperature [16], we determined T in the following way. Assuming that the microsphere diameter and its distance to the surface is known, we calculated the temperature by varying T until the experimentally measured value for the drag coefficient γ_{ex} at $f = 0$ was equal to the theoretically expected one: $\gamma_{\text{ex}} - \gamma = k_B T/(\beta^2 D^{\text{volt}}) - 6\pi\eta(T)R/[1 - (9/16)(R/\ell)] = 0$. Since the viscosity $\eta(T)$ is a nonlinear function of temperature, we numerically solved for T.
[27] Up to which frequency noise is reduced depends on the exponential term in Eq. (2). Setting the real part of the exponent to -2, meaning a reduction to $e^{-2} \approx 14\%$ and assuming $\ell \gg R$, results in the stated estimate for the frequency f_ℓ.
[28] T. Franosch, M. Grimm, M. Belushkin, F. Mor, G. Foffi, L. Forró, and S. Jeney, Nature **478**, 85 (2011).
[29] J. C. M. Gebhardt, T. Bornschlögl, and M. Rief, Proc. Natl. Acad. Sci. U.S.A. **107**, 2013 (2010).
[30] M. Hinczewski, Y. von Hansen, and R. R. Netz, Proc. Natl. Acad. Sci. U.S.A. **107**, 21493 (2010).
[31] http://en.wikipedia.org/wiki/Colors_of_noise, modified at 16:02 on 6 August 2011.
[32] S. F. Nørrelykke and H. Flyvbjerg, Rev. Sci. Instrum. **81**, 075103 (2010).